Journal of
Mechanics of
Materials and Structures

NONUNIFORM INTERFACIAL SLIP IN FIBROUS COMPOSITES

Xu Wang

NONUNIFORM INTERFACIAL SLIP IN FIBROUS COMPOSITES

XU WANG

We consider a solitary circular elastic inclusion bonded to an infinite elastic matrix through a linear viscous interface. Here the viscous interface with vanishing thickness can simulate the Nabarro–Herring or Coble creep of a thin interphase layer between the fiber and the matrix. The interface drag parameter is varied along the interface to reflect the real thickening and thinning of the interphase layer. In particular, we consider a special form of the interface function that yields closed-form solutions in terms of elementary functions under four loading conditions: the matrix is subjected to remote uniform antiplane shearing; a screw dislocation is located in the matrix; a screw dislocation is located inside the inclusion; and uniform eigenstrains are imposed on the inclusion.

Our results show that a nonuniform interface parameter will induce an intrinsically nonuniform stress field inside the inclusion when the matrix is subjected to remote uniform shearing or when uniform eigenstrains are imposed on the inclusion, and will also result in a noncentral image force acting on the screw dislocation. In addition, the nonuniformity of the interface will increase the characteristic time of the composite. More interestingly our results show that there coexist at the same time a transient stable and another transient unstable equilibrium positions for a screw dislocation in the matrix when the viscous interface is extremely nonuniform and when the inclusion is stiffer than the matrix. Also discussed is the overall time-dependent shear modulus of the fibrous composite by using the Mori–Tanaka mean-field method.

Notation

w	Out-of-plane displacement
σ_{zx}, σ_{zy}	Stress components in the Cartesian coordinate system
σ_{zr}, $\sigma_{z\theta}$	Stress components in the polar coordinate system
γ_{zx}, γ_{zy}	Engineering shear strains
μ	Shear modulus
R	Radius of the circular inclusion
$\beta(\theta)$	Nonuniform interface drag parameter
t	Time
z	Complex variable
c	Volume fraction of the fiber
b	Burgers vector
F_r, F_θ	Image force components on the dislocation in polar coordinates

Superscript [1] and [2] denote, respectively, the physical quantities in the inclusion and matrix.

1. Introduction

In fibrous composites an interphase layer is often introduced between the inclusion (fiber) and the matrix to improve the attachment between the inclusion and the matrix, and to reduce the material mismatch induced stress concentration at the interface (see [Ru 1999] and the references cited therein). Under some conditions (for example at high temperatures), the creep behavior of the interphase layer should be considered [Kim and McMeeking 1995; Fan and Wang 2003]. It is further assumed that the interphase layer is creeping in the linear region controlled by Nabarro–Herring or Coble creep which is diffusion-controlled [Frost and Ashby 1982; Kim and McMeeking 1995]. The creep behavior of the interphase layer can be described by $\tau = \eta\dot{\gamma}$, where τ is the shear stress, η is the viscosity and $\dot{\gamma}$ is the shear strain rate. In this research it is assumed that the thickness h of the interphase layer is much smaller that the radius R of the fiber, that is, $h \ll R$. As a result, $\dot{\gamma} = \dot{\delta}/h$, where $\dot{\delta}$ is the sliding velocity (the differentiation of the relative sliding with respect to the time t). Consequently the slip boundary condition on the interface can be written as $\tau = \beta\dot{\delta}$, with $\beta = \eta/h \geq 0$ being the interface drag parameter, which is identical to the constitutive law for a viscous interface. If we take into consideration the fact that the thickening and thinning of the interphase layer is quite possible during creep flow [Kim and McMeeking 1995], then $\beta = \beta(\theta)$, with θ being the polar angle, is nonuniform along the interface. The aim of this research is to investigate the influence of the nonuniformity of $\beta = \beta(\theta)$ on the response of the fibrous composite with a viscous (or time-dependent sliding) interface. In general it is only possible to derive series form solutions when $\beta(\theta)$ takes an arbitrary form. Here we focus on the special form $1/\beta(\theta) = a_0 + a_1 e^{i\theta} + \bar{a}_1 e^{-i\theta}$, with $a_0 \geq 2|a_1|$, for which closed-form solutions in terms of elementary functions still exist.

2. Basic formulae

We consider a domain in $\mathbb{R}^2$, infinite in extent, containing a solitary circular elastic inclusion of radius R with elastic properties different from those of the surrounding matrix (Figure 1). The linearly elastic materials occupying the inclusion and the matrix are assumed to be homogeneous and isotropic with associated shear moduli μ_1 and μ_2. In this research we ignore the inertia effect for both the inclusion and the matrix, and the two-phase composite is under antiplane shear deformations. Consequently the
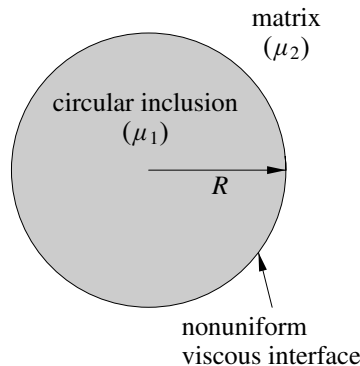
Figure 1. A circular elastic inclusion bonded to an infinite elastic matrix through a nonuniform viscous interface.

out-of-plane displacement w, the stress components σ_{zx}, σ_{zy} in the Cartesian coordinate system, and the stress components σ_{zr}, $\sigma_{z\theta}$ in the polar coordinate system can be expressed in terms of a single analytic function $f(z, t)$ as

$$w = \operatorname{Im} f(z, t), \tag{1}$$

$$\sigma_{zy} + i\sigma_{zx} = \mu f'(z, t), \tag{2}$$

$$\sigma_{z\theta} + i\sigma_{zr} = \mu \frac{z}{|z|} f'(z, t), \tag{3}$$

where t is the real time variable, whilst $z = x + iy = re^{i\theta}$ is the complex variable, and $f'(z, t) = \partial f(z, t)/\partial z$. The appearance of the real time variable t in the analytic function f is due to the influence of the viscous interface between the inclusion and the surrounding matrix.

3. General solutions

In this section we will derive general solutions for the loading case in which the matrix is subjected to an arbitrary type singularity (for example, remote uniform loading or a screw dislocation in the matrix). It follows from the Introduction that the boundary conditions on the interface can be expressed as

$$\sigma_{zr}^{(1)} = \sigma_{zr}^{(2)} = \beta(\theta)(\dot{w}^{(2)} - \dot{w}^{(1)}), \quad r = R \text{ and } t > 0, \tag{4}$$

where the interface drag parameter $\beta(\theta)$ (≥ 0) is a periodic function of the polar angle θ. In this research it is further assumed that $\beta(\theta)$ takes the following special form:

$$\frac{1}{\beta(\theta)} = a_0 + a_1 e^{i\theta} + \bar{a}_1 e^{-i\theta}, \tag{5}$$

where $a_0 \geq 2|a_1|$ to ensure a nonnegative value of $\beta(\theta)$.

The boundary conditions in (4) can also be equivalently expressed in terms of $f_1(z, t)$ defined in the circular inclusion and $f_2(z, t)$ defined in the matrix as

$$\mu_1 f_1^+(z, t) + \mu_1 \bar{f}_1^- \left(\frac{R^2}{z}, t\right) = \mu_2 f_2^-(z, t) + \mu_2 \bar{f}_2^+ \left(\frac{R^2}{z}, t\right), \tag{6}$$

$$\dot{f}_2^-(z, t) - \dot{\bar{f}}_2^+ \left(\frac{R^2}{z}, t\right) - \dot{f}_1^+(z, t) + \dot{\bar{f}}_1^- \left(\frac{R^2}{z}, t\right) = \frac{\mu_1}{\beta(\theta)R} \left(z f_1'^+(z, t) - \frac{R^2}{z} \bar{f}_1'^- \left(\frac{R^2}{z}, t\right)\right) \quad (|z| = R).$$

It follows from $(6)_1$ that

$$f_2(z, t) = \frac{\mu_1}{\mu_2} \bar{f}_1 \left(\frac{R^2}{z}, t\right) + f_0(z) - \bar{f}_0 \left(\frac{R^2}{z}\right), \quad \bar{f}_2 \left(\frac{R^2}{z}, t\right) = \frac{\mu_1}{\mu_2} f_1(z, t) + \bar{f}_0 \left(\frac{R^2}{z}\right) - f_0(z), \tag{7}$$

where $f_0(z)$, which is time-independent, is the complex potential for a singularity in an infinite homogeneous material with shear modulus μ_2. For example, when the matrix is subjected to uniform loading at infinity, $f_0(z)$ is given by

$$f_0(z) = \frac{\sigma_{zy}^\infty + i\sigma_{zx}^\infty}{\mu_2} z. \tag{8}$$

When the matrix is only subjected to a screw dislocation with Burgers vector b at $z = z_0 = x_0 + i y_0$, then $f_0(z)$ is

$$f_0(z) = \frac{b}{2\pi} \ln(z - z_0). \tag{9}$$

Substituting (7) into (6)$_2$ and eliminating $f_2^-(z)$ and $\bar{f}_2^+(R^2/z)$, we finally arrive at

$$\dot{f}_1^+(z, t) + \frac{\mu_1 \mu_2}{R\eta(\theta)(\mu_1 + \mu_2)} z f_1'^+(z, t) = \dot{\bar{f}}_1^-\left(\frac{R^2}{z}, t\right) + \frac{\mu_1 \mu_2}{R\beta(\theta)(\mu_1 + \mu_2)} \frac{R^2}{z} \bar{f}_1'^-\left(\frac{R^2}{z}, t\right)$$
$$(|z| = R). \tag{10}$$

In view of the expression (5) for $\beta(\theta)$, it follows that the left-hand side of (10) is analytic within the circle $|z| = R$, while the right-hand side of (10) is analytic outside the circle, including the point at infinity. By applying Liouville's theorem, we arrive at the following partial differential equation for $f_1(z, t)$:

$$\dot{f}_1(z, t) + \frac{\mu_1 \mu_2}{R\beta(\theta)(\mu_1 + \mu_2)} z f_1'(z, t) = 0, \quad (|z| < R). \tag{11}$$

The above equation is still difficult to solve in its present form in view of the fact that $\beta(\theta)$ is varied along the circular interface. In order to solve the above equation, we introduce the following conformal mapping function

$$z = m(\zeta) = \frac{\zeta - \rho}{(\bar{\rho}/R^2)\zeta - 1}, \tag{12}$$

where

$$\rho = -\frac{2\bar{a}_1}{a_0 + \sqrt{a_0^2 - 4|a_1|^2}} R \quad (|\rho| < R). \tag{13}$$

Now (11) can be simplified in the ζ-domain as

$$\dot{f}_1(\zeta, t) + \lambda \zeta f_1'(\zeta, t) = 0 \quad (|\zeta| < R), \tag{14}$$

where

$$\lambda = \frac{\sqrt{a_0^2 - 4|a_1|^2} \mu_1 \mu_2}{R(\mu_1 + \mu_2)}. \tag{15}$$

In writing (14), for convenience $f_1(z, t) = f_1(m(\zeta), t) = f_1(\zeta, t)$ has been adopted. It is observed that not only a_0 but also a_1, which characterizes the nonuniformity of the interface, enters the expression of λ, which is the inverse of the characteristic time t_0. The nonuniformity of the interface will increase the characteristic time. The general solution to (14) can be easily obtained as $f_1(\zeta, t) = f_1(\exp(-\lambda t)\zeta, 0)$. Finally, the general solution in the original z-plane can be given as

$$f_1(z, t) = f_1\left(\frac{z(R^2 \exp(-\lambda t) - \rho\bar{\rho}) + \rho R^2(1 - \exp(-\lambda t))}{z\bar{\rho}(\exp(-\lambda t) - 1) + R^2 - \rho\bar{\rho}\exp(-\lambda t)}, 0\right) \quad (|z| < R), \tag{16}$$

which indicates that once the initial value $f_1(z, 0)$ is known, it is enough to replace the complex variable z by

$$\frac{z(R^2 \exp(-\lambda t) - \rho\bar{\rho}) + \rho R^2 - \rho R^2 \exp(-\lambda t)}{z\bar{\rho}(\exp(-\lambda t) - 1) + R^2 - \rho\bar{\rho}\exp(-\lambda t)}$$

to arrive at $f_1(z, t)$.

At the initial time $t = 0$ the interface is a perfect one due to the fact that at $t = 0$ the displacement across the interface has no time to experience any jump [Fan and Wang 2003]. As a result we can obtain the initial value $f_1(z, 0)$ as

$$f_1(z, 0) = \frac{2\mu_2}{\mu_1 + \mu_2} f_0(z). \tag{17}$$

Then $f_1(z, t)$ in (16) can be more specifically expressed as

$$f_1(z, t) = \frac{2\mu_2}{\mu_1 + \mu_2} f_0\left(\frac{z(R^2 \exp(-\lambda t) - \rho\bar{\rho}) + \rho R^2(1 - \exp(-\lambda t))}{z\bar{\rho}(\exp(-\lambda t) - 1) + R^2 - \rho\bar{\rho}\exp(-\lambda t)}\right) \quad (|z| < R). \tag{18}$$

Substituting this into $(7)_1$, we arrive at the expression of $f_2(z, t)$ as

$$f_2(z, t) = \frac{2\mu_1}{\mu_1 + \mu_2} \overline{f_0\left(\frac{\bar{z}\rho R^2(1 - \exp(-\lambda t)) + R^2(R^2 \exp(-\lambda t) - \rho\bar{\rho})}{\bar{z}(R^2 - \rho\bar{\rho}\exp(-\lambda t)) + \bar{\rho}R^2(\exp(-\lambda t) - 1)}\right)} + f_0(z) - \bar{f}_0\left(\frac{R^2}{z}\right)$$
$$(|z| > R). \tag{19}$$

4. Specific results for an arbitrary singularity in the matrix

We now address some specific loadings to demonstrate the general solutions obtained.

4.1. *Remote uniform loading.* When the matrix is subjected to uniform loading, it follows from (8) for the specific expression of $f_0(z)$ and the general solutions (18) and (19) that

$$f_1(z, t) = \frac{2(\sigma_{zy}^\infty + i\sigma_{zx}^\infty)}{\mu_1 + \mu_2} \frac{z(R^2 \exp(-\lambda t) - \rho\bar{\rho}) + \rho R^2(1 - \exp(-\lambda t))}{z\bar{\rho}(\exp(-\lambda t) - 1) + R^2 - \rho\bar{\rho}\exp(-\lambda t)} \quad (|z| < R), \tag{20}$$

$$f_2(z, t) = \frac{2\mu_1(\sigma_{zy}^\infty - i\sigma_{zx}^\infty)}{\mu_2(\mu_1 + \mu_2)} \frac{z\bar{\rho}R^2(1 - \exp(-\lambda t)) + R^2(R^2 \exp(-\lambda t) - \rho\bar{\rho})}{z(R^2 - \rho\bar{\rho}\exp(-\lambda t)) + \rho R^2(\exp(-\lambda t) - 1)}$$
$$- \frac{\sigma_{zy}^\infty - i\sigma_{zx}^\infty}{\mu_2} \frac{R^2}{z} + \frac{\sigma_{zy}^\infty + i\sigma_{zx}^\infty}{\mu_2} z \quad (|z| > R). \tag{21}$$

Thus the time-dependent stresses in the two-phase composite can be easily obtained as

$$\sigma_{zy}^{(1)} + i\sigma_{zx}^{(1)} = \frac{2\mu_1(\sigma_{zy}^\infty + i\sigma_{zx}^\infty)}{\mu_1 + \mu_2} \frac{(R^2 - \rho\bar{\rho})^2 \exp(-\lambda t)}{(z\bar{\rho}(\exp(-\lambda t) - 1) + R^2 - \rho\bar{\rho}\exp(-\lambda t))^2} \quad (|z| < R), \tag{22}$$

$$\sigma_{zy}^{(2)} + i\sigma_{zx}^{(2)} = (\sigma_{zy}^\infty - i\sigma_{zx}^\infty)\left(\frac{R^2}{z^2} - \frac{2\mu_1}{(\mu_1 + \mu_2)} \frac{R^2(R^2 - \rho\bar{\rho})^2 \exp(-\lambda t)}{(z(R^2 - \rho\bar{\rho}\exp(-\lambda t)) + \rho R^2(\exp(-\lambda t) - 1))^2}\right)$$
$$+ \sigma_{zy}^\infty + i\sigma_{zx}^\infty \quad (|z| > R). \tag{23}$$

Clearly the internal stress field is intrinsically nonuniform when $t > 0$ due to the nonuniformity of the sliding interface ($\rho \neq 0$). To highlight this, we show in Figure 2 the nonuniform distributions of the internal stress components

$$\tilde{\sigma}_{zy} = \frac{\mu_1 + \mu_2}{2\mu_1} \frac{\sigma_{zy}^{(1)}}{\sigma_{zy}^\infty} \quad \text{and} \quad \tilde{\sigma}_{zx} = \frac{\mu_1 + \mu_2}{2\mu_1} \frac{\sigma_{zx}^{(1)}}{\sigma_{zy}^\infty}$$
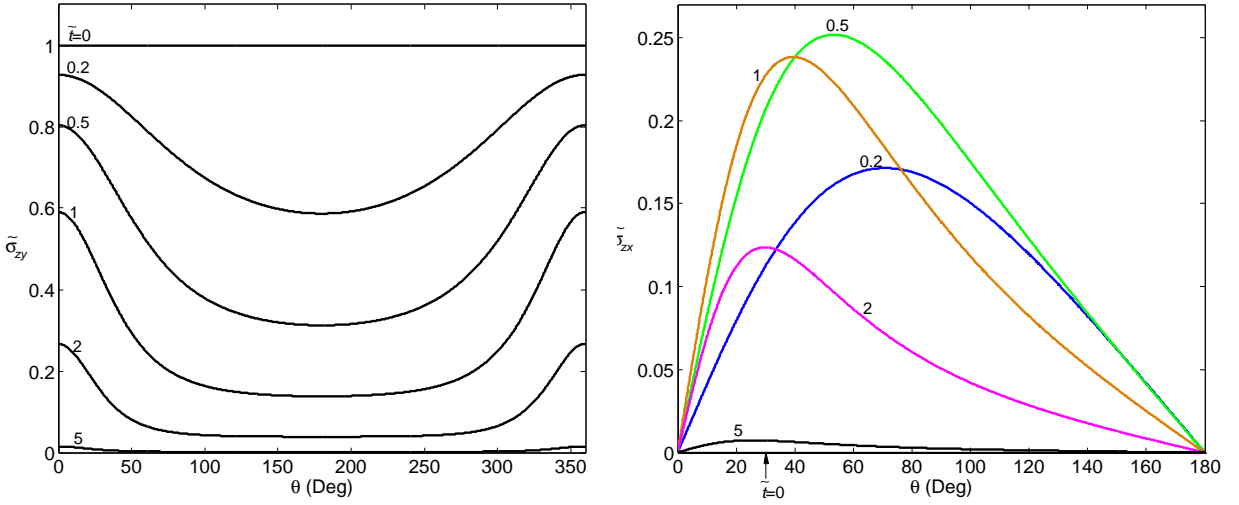
Figure 2. Nonuniform distribution of the internal stress components $\tilde{\sigma}_{zy}$ and $\tilde{\sigma}_{zx}$ along the circular interface $z = Re^{i\theta}$ at times $\tilde{t} = \lambda t = 0, 0.2, 0.5, 1, 2, 5$, with $\rho = 0.5R$, when the matrix is only subjected to σ_{zy}^{∞}.

along the circular interface $z = Re^{i\theta}$ at six different times $\tilde{t} = \lambda t = 0, 0.2, 0.5, 1, 2, 5$ with $\rho = 0.5R$ when the matrix is only subjected to σ_{zy}^{∞}. It is clearly observed that the internal stresses are nonuniformly distributed along the interface when $t > 0$ and that nonzero $\sigma_{zx}^{(1)}$ will also be induced by σ_{zy}^{∞} when $t > 0$ (notice that σ_{zy}^{∞} will not induce the stress component $\sigma_{zx}^{(1)}$ when the interface is uniform). In addition the internal stress level of $\tilde{\sigma}_{zy}$ will monotonically decrease as the time evolves, whilst that of $\tilde{\sigma}_{zx}$ attains a maximum value at a certain moment. When $t \to \infty$ the internal stresses approach zero since the fact that the viscous interface will finally become a free-sliding one which does not sustain any shear force.

The time-dependent average stresses $\overline{\sigma_{zy}^{(1)}}$ and $\overline{\sigma_{zx}^{(1)}}$ within the circular inclusion, which are equivalent to the stresses at the center of the circular inclusion [Ru and Schiavone 1997], can be obtained as

$$\sigma = \frac{\overline{\sigma_{zy}^{(1)}} + i\overline{\sigma_{zx}^{(1)}}}{\sigma_{zy}^{\infty} + i\sigma_{zx}^{\infty}} = \frac{2\mu_1}{\mu_1 + \mu_2} \frac{(R^2 - \rho\bar{\rho})^2 \exp(-\lambda t)}{(R^2 - \rho\bar{\rho}\exp(-\lambda t))^2}, \tag{24}$$

which is a monotonically decreasing function of the time t.

The displacement jump across the circular interface can be obtained as

$$\begin{aligned}
\Delta w &= w^{(2)} - w^{(1)} \\
&= \frac{2R|Re^{i\theta} - \rho|^2(1 - \exp(-\lambda t))}{\mu_2} \operatorname{Im} \frac{\sigma_{zy}^{\infty} + i\sigma_{zx}^{\infty}}{e^{-i\theta}(R^2 - \rho\bar{\rho}\exp(-\lambda t)) - R\bar{\rho}(1 - \exp(-\lambda t))}.
\end{aligned} \tag{25}$$

The obtained results for an isolated inclusion can be further employed to predict the effective properties of a two-phase composite consisting of equal-sized circular isotropic cylinders (with shear modulus μ_1) of radius R randomly dispersed in a homogeneous isotropic matrix of shear modulus μ_2. Here we adopt the Mori–Tanaka mean field method [Mori and Tanaka 1973; He and Lim 2001] to derive the effective

properties of the composite. Somewhat to our surprise, we find that the overall behavior of the fibrous composite under longitudinal shearing is still *isotropic* even though the interface drag parameter $\beta(\theta)$ is varied along the interface. In addition the overall constitutive law for the fibrous composite can be represented by

$$\langle \sigma_{zy} \rangle = \mu_c \langle \gamma_{zy} \rangle, \qquad \langle \sigma_{zx} \rangle = \mu_c \langle \gamma_{zx} \rangle, \tag{26}$$

where $\langle * \rangle$ stands for the average value, μ_c stands for the time-dependent effective shear modulus. Here $\gamma_{zy} = \partial w / \partial y$ and $\gamma_{zx} = \partial w / \partial x$ are the engineering shear strains in view of the fact that the in-plane displacements are zero.

In order to describe the overall behavior of the composite, we focus on a representative volume element (RVE). In addition we assume that the RVE is subjected to the antiplane shearing σ_{zy}^∞. The volume-averaged values within the RVE can be proved to be [He and Lim 2001]

$$\langle \sigma_{zy} \rangle = c \langle \sigma_{zy} \rangle_f + (1-c) \langle \sigma_{zy} \rangle_m,$$
$$\langle \gamma_{zy} \rangle = c \langle \gamma_{zy} \rangle_f + (1-c) \langle \gamma_{zy} \rangle_m + \frac{c}{\pi R^2} \int_l \Delta w \hat{n}_2 dl, \tag{27}$$

where c is the volume fraction of the fiber, $\langle \ \rangle_f$ and $\langle \ \rangle_m$ refer to the averages over volumes of the fiber and matrix respectively, the line integral is taken along the perimeter l of a typical fiber, Δw is the displacement jump across the interface, and $\hat{n}_2$ is the y-component of the unit normal vector on the interface in the outward direction with respect to the fiber. In addition $\langle \sigma_{zy} \rangle = \sigma_{zy}^\infty$. Here the Mori–Tanaka mean-field approximation is adopted to evaluate $\langle \sigma_{zy} \rangle_f$. Under this approximation $\langle \sigma_{zy} \rangle_f$ is equal to the average value of σ_{zy} in an isolated fiber embedded in an infinitely extended matrix that is subjected to the shear stress $\langle \sigma_{zy} \rangle_m$ at infinity. Then it follows from (24) and $(27)_1$ that

$$\langle \sigma_{zy} \rangle_m = \frac{\sigma_{zy}^\infty}{1 - \left(c - c \dfrac{2\mu_1}{\mu_1 + \mu_2} \dfrac{(R^2 - \rho \bar{\rho})^2 \exp(-\lambda t)}{(R^2 - \rho \bar{\rho} \exp(-\lambda t))^2} \right)}. \tag{28}$$

The average shear strain in the fiber and in the matrix can be found as

$$\langle \gamma_{zy} \rangle_f = \frac{\langle \sigma_{zy} \rangle_f}{\mu_1}, \qquad \langle \gamma_{zy} \rangle_m = \frac{\langle \sigma_{zy} \rangle_m}{\mu_2}, \tag{29}$$

and the surface integral in $(27)_2$ can be finally carried out as follows

$$\frac{1}{\pi R^2} \int_l \Delta w n_2 dl = 2 \langle \sigma_{zy} \rangle_m \frac{(1 - \exp(-\lambda t))}{\mu_2} \frac{R^4 - |\rho|^4 \exp(-\lambda t)}{(R^2 - |\rho|^2 \exp(-\lambda t))^2}. \tag{30}$$

Equation (25) and the residue theorem have been utilized to derive (30). By using (28), (29) and (30), Equation $(27)_2$ can be finally expressed as

$$\langle \gamma_{zy} \rangle = \frac{1 + c \left(1 - \dfrac{2\mu_1}{\mu_1 + \mu_2} \dfrac{(R^2 - |\rho|^2)^2 \exp(-\lambda t)}{(R^2 - |\rho|^2 \exp(-\lambda t))^2} \right)}{1 - c \left(1 - \dfrac{2\mu_1}{\mu_1 + \mu_2} \dfrac{(R^2 - |\rho|^2)^2 \exp(-\lambda t)}{(R^2 - |\rho|^2 \exp(-\lambda t))^2} \right)} \frac{\sigma_{zy}^\infty}{\mu_2}, \tag{31}$$

Comparison of (26) with (31) will immediately lead to the time-dependent effective modulus as

$$
\mu_c = \mu_2 \frac{1 - c\left(1 - \dfrac{2\mu_1}{\mu_1 + \mu_2} \dfrac{(R^2 - |\rho|^2)^2 \exp(-\lambda t)}{(R^2 - |\rho|^2 \exp(-\lambda t))^2}\right)}{1 + c\left(1 - \dfrac{2\mu_1}{\mu_1 + \mu_2} \dfrac{(R^2 - |\rho|^2)^2 \exp(-\lambda t)}{(R^2 - |\rho|^2 \exp(-\lambda t))^2}\right)},
\tag{32}
$$

which will reduce to the value obtained by [He and Lim 2001] when $\rho = 0$ for a homogeneous interface.

4.2. *A screw dislocation in the matrix.* When the matrix is only subjected to a screw dislocation with Burgers vector b at $z = z_0$, it follows from (9) for the specific expression of $f_0(z)$ and the general solutions (18) and (19) that

$$
f_1(z, t) = \frac{\mu_2 b}{\pi(\mu_1 + \mu_2)} \ln\left(\frac{z(R^2 \exp(-\lambda t) - \rho\bar{\rho}) + \rho R^2(1 - \exp(-\lambda t))}{z\bar{\rho}(\exp(-\lambda t) - 1) + R^2 - \rho\bar{\rho}\exp(-\lambda t)} - z_0\right) \quad (|z| < R), \tag{33}
$$

$$
f_2(z, t) = \frac{\mu_1 b}{\pi(\mu_1 + \mu_2)} \ln\left(\frac{z\bar{\rho}R^2(1 - \exp(-\lambda t)) + R^2(R^2 \exp(-\lambda t) - \rho\bar{\rho})}{z(R^2 - \rho\bar{\rho}\exp(-\lambda t)) + \rho R^2(\exp(-\lambda t) - 1)} - \bar{z}_0\right)
$$
$$
+ \frac{b}{2\pi} \ln\frac{z(z - z_0)}{\bar{z}_0 z - R^2} \quad (|z| > R). \tag{34}
$$

Equation (33) implies that the solution in the inclusion can be considered as the superposition of the following two moving dislocations in a homogeneous infinite elastic plane with the shear modulus μ_1:

(i) a dislocation $\dfrac{2\mu_2}{\mu_1 + \mu_2} b$ located at the moving singular point

$$
z = \frac{z_0(R^2 - \rho\bar{\rho}\exp(-\lambda t)) - \rho R^2(1 - \exp(-\lambda t))}{(R^2 \exp(-\lambda t) - \rho\bar{\rho}) - z_0\bar{\rho}(\exp(-\lambda t) - 1)},
$$

which originates from $z = z_0$ and moves toward $z = R^2/\bar{\rho}$;

(ii) a dislocation $-\dfrac{2\mu_2}{\mu_1 + \mu_2} b$ located at the moving singular point

$$
z = \frac{R^2 - \rho\bar{\rho}\exp(-\lambda t)}{\bar{\rho}(1 - \exp(-\lambda t))},
$$

which originates from $z = \infty$ and moves toward $z = R^2/\bar{\rho}$.

The two moving image dislocations (or more precisely a moving dislocation dipole), both of which are located outside the inclusion, will finally converge to the same point $z = R^2/\bar{\rho}$, as seen in Figure 3. The sum of the two moving dislocations is always zero.

Equation (34) implies that the solution in the matrix can be considered as the superposition of the following three static dislocations and two moving dislocations in a homogeneous infinite elastic plane with the shear modulus μ_2:

(i) a dislocation b located at the original static singular point $z = z_0$;

(ii) a dislocation $-b$ located at the static singular point $z = R^2/\bar{z}_0$;

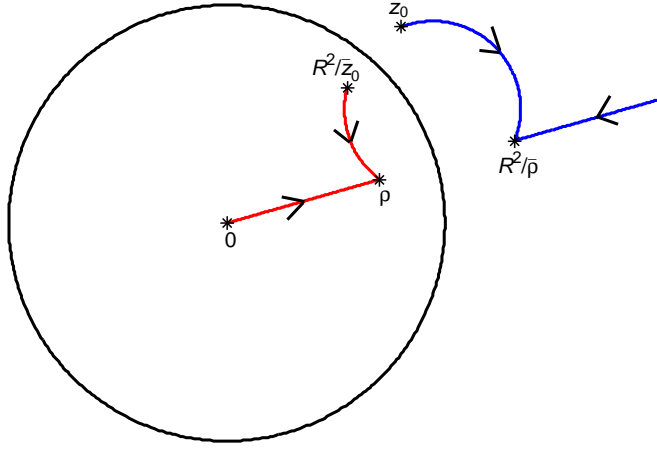(iii) a dislocation b located at the static singular point $z = 0$;

Figure 3. Loci of the moving image dislocations when the original dislocation is located in the matrix. The image dislocations outside the circle $r = R$ are those for the inclusion; those within the circle $r = R$ are for the matrix.

(iv) a dislocation $\dfrac{2\mu_1}{\mu_1 + \mu_2} b$ located at the moving singular point

$$z = \frac{\bar{z}_0 \rho R^2 (\exp(-\lambda t) - 1) - R^2 (R^2 \exp(-\lambda t) - \rho \bar{\rho})}{\bar{\rho} R^2 (1 - \exp(-\lambda t)) - \bar{z}_0 (R^2 - \rho \bar{\rho} \exp(-\lambda t))},$$

which originates from $z = R^2/\bar{z}_0$ and moves toward $z = \rho$;

(v) a dislocation $-\dfrac{2\mu_1}{\mu_1 + \mu_2} b$ located at the moving singular point

$$z = \frac{\rho R^2 (1 - \exp(-\lambda t))}{R^2 - \rho \bar{\rho} \exp(-\lambda t)},$$

which originates from $z = 0$ and moves toward $z = \rho$.

Except for the original dislocation at $z = z_0$, all the other four image dislocations are located within the inclusion. The two moving dislocations (or more precisely a moving dislocation dipole) will finally converge to the same point $z = \rho$, as also illustrated in Figure 3. The sum of these five dislocations is b.

In the polar coordinate system, the time-dependent image force acting on the screw dislocation is (see [Lazar 2007])

$$F_r - i F_\theta$$

$$= \frac{\mu_1 \mu_2 b^2}{\pi (\mu_1 + \mu_2)} \frac{R^2 (R^2 - |\rho|^2)^2 \exp(-\lambda t)}{|z_0|^2 (R^2 - |\rho|^2 \exp(-\lambda t)) - 2 \operatorname{Re}(z_0 \bar{\rho}) R^2 (1 - \exp(-\lambda t)) - R^2 (R^2 \exp(-\lambda t) - |\rho|^2)}$$

$$\times \frac{1}{|z_0|((R^2 - |\rho|^2 \exp(-\lambda t)) + z_0^{-1} \rho R^2 (\exp(-\lambda t) - 1))} - \frac{\mu_2 b^2}{2\pi} \frac{R^2}{|z_0|(|z_0|^2 - R^2)}, \quad (35)$$

where F_r and F_θ are respectively the radial and tangential components of the image force. When $\rho = 0$ for a homogeneous viscous interface, this reduces to that derived in [Wang et al. 2008]. On the other hand, when $t = 0$, the expression above reduces to Dundurs' classical solution [1967] for a perfect interface.
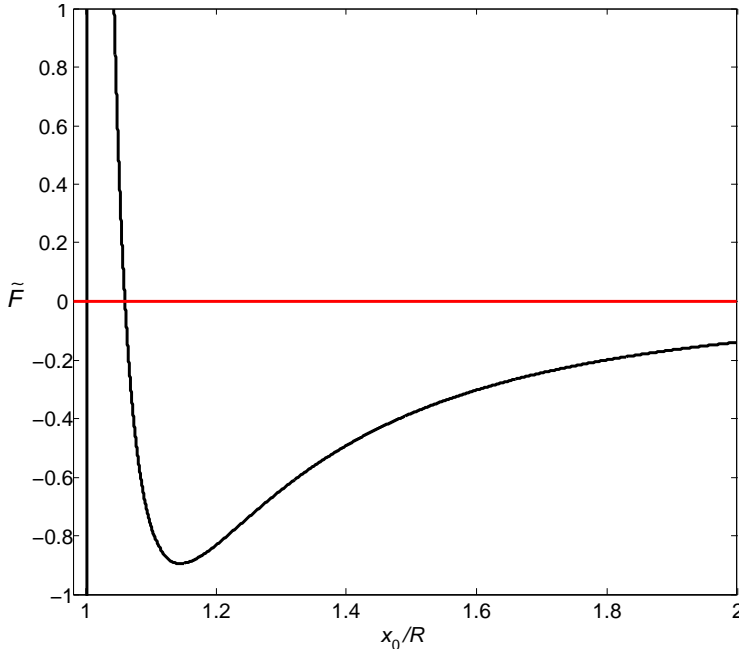
Figure 4. Distribution of the image force $\tilde{F}$ on a screw dislocation located on the positive x-axis in the matrix when $\mu_1 = 3\mu_2$, $\rho = 0.98R$ and $\lambda t = 0.2$.

It is observed that in general the image force is not a central force due to the existence of the nonzero tangential component F_θ. This noncentral image force is solely caused by the nonuniformity of the viscous interface (that is, $\rho \neq 0$). Only when $\mathrm{Arg}(z_0) = \mathrm{Arg}(\rho)$ or $\mathrm{Arg}(z_0) = \mathrm{Arg}(\rho) - \pi$ will the image force be a central one with $F_\theta = 0$.

It has been found that there exists a transient unstable equilibrium position ($F_r = F_\theta = 0$) for a screw dislocation interacting with a homogeneous viscous interface when the inclusion is stiffer than the matrix [Wang et al. 2008]. Our present results show that when the nonuniformity of the interface is extremely serious ($|\rho| \rightarrow R$) and when the inclusion is stiffer than the matrix, a transient stable equilibrium position and another transient unstable equilibrium position may exist at the same time. To highlight this unique feature, we show in Figure 4 the distribution of the image force $\tilde{F} = (2\pi R/\mu_2 b^2) F_r$, on a screw dislocation located on the positive x-axis in the matrix when $\mu_1 = 3\mu_2$, $\rho = 0.98R$ and $\lambda t = 0.2$. It is observed from (35) that $F_\theta = 0$ when ρ and z_0 are both real. It can be seen in Figure 4 that $x_0 = 1.0022R$, which is extremely close to the interface, is a transient unstable equilibrium position, whilst $x_0 = 1.0598R$, which is further away from the interface, is a transient stable equilibrium position.

5. Other loading conditions

The general solutions derived in Section 3 are only valid for an arbitrary type singularity located in the matrix. In fact the method in Section 3 can be extended to other loading conditions. In the following we will address two other type loading conditions: (i) a screw dislocation inside the inclusion; (ii) uniform eigenstrains imposed on the inclusion.

5.1. *A screw dislocation inside the inclusion.* The analysis of a screw dislocation inside the inclusion is similar to, but a little bit more difficult than, the above analysis of a screw dislocation in the matrix. Here the specific intermediate procedure will be suppressed. When the screw dislocation is located at $z = z_0$ in the inclusion, the two analytic functions can be finally obtained as

$$f_1(z, t) = \frac{\mu_2 b}{\pi(\mu_1 + \mu_2)} \ln\left(\frac{z\bar{\rho}R^2(1 - \exp(\lambda t)) + R^2(R^2 \exp(\lambda t) - \rho\bar{\rho})}{z(R^2 - \rho\bar{\rho}\exp(\lambda t)) + \rho R^2(\exp(\lambda t) - 1)} - \bar{z}_0\right)$$

$$- \frac{\mu_2 b}{\pi(\mu_1 + \mu_2)} \ln\frac{z\bar{\rho}R^2(1 - \exp(\lambda t)) + R^2(R^2 \exp(\lambda t) - \rho\bar{\rho})}{z(R^2 - \rho\bar{\rho}\exp(\lambda t)) + \rho R^2(\exp(\lambda t) - 1)} + \frac{b}{2\pi} \ln\frac{z - z_0}{\bar{z}_0 z - R^2} \quad (|z| < R), \quad (36)$$

$$f_2(z, t) = \frac{\mu_1 b}{\pi(\mu_1 + \mu_2)} \ln\left(\frac{z(R^2 \exp(\lambda t) - \rho\bar{\rho}) + \rho R^2(1 - \exp(\lambda t))}{z\bar{\rho}(\exp(\lambda t) - 1) + R^2 - \rho\bar{\rho}\exp(\lambda t)} - z_0\right)$$

$$- \frac{\mu_1 b}{\pi(\mu_1 + \mu_2)} \ln\frac{z(R^2 \exp(\lambda t) - \rho\bar{\rho}) + \rho R^2(1 - \exp(\lambda t))}{z\bar{\rho}(\exp(\lambda t) - 1) + R^2 - \rho\bar{\rho}\exp(\lambda t)} + \frac{b}{2\pi} \ln z \quad (|z| > R). \quad (37)$$

Equation (36) implies that the solution in the inclusion can be considered as the superposition of the following two static dislocations and two moving dislocations in a homogeneous infinite elastic plane with the shear modulus μ_1:

(i) a dislocation b located at the original static singular point $z = z_0$;

(ii) a dislocation $-b$ located at the static singular point $z = R^2/\bar{z}_0$;

(iii) a dislocation $\dfrac{2\mu_2}{\mu_1 + \mu_2} b$ located at the moving singular point

$$z = \frac{\bar{z}_0 \rho R^2(\exp(\lambda t) - 1) - R^2(R^2 \exp(\lambda t) - \rho\bar{\rho})}{\bar{\rho}R^2(1 - \exp(\lambda t)) - \bar{z}_0(R^2 - \rho\bar{\rho}\exp(\lambda t))},$$

which originates from $z = R^2/\bar{z}_0$ and moves toward $z = (R^2/\bar{\rho})$;

(iv) a dislocation $-\dfrac{2\mu_2}{\mu_1 + \mu_2} b$ located at the moving singular point

$$z = \frac{R^2(R^2 \exp(\lambda t) - \rho\bar{\rho})}{\bar{\rho}R^2(\exp(\lambda t) - 1)},$$

which originates from $z = \infty$ and moves toward $z = R^2/\bar{\rho}$.

Except for the original dislocation at $z = z_0$, all other image dislocations are located outside the inclusion. The two moving dislocations (or more precisely a moving dislocation dipole) will finally converge to the same point $z = R^2/\bar{\rho}$, as seen in Figure 5. The sum of these four dislocations is zero.

Equation (37) implies that the solution in the matrix can be considered as the superposition of the following one static dislocation and two moving dislocations in a homogeneous infinite elastic plane with shear modulus μ_2:

(i) a dislocation b located at the static singular point $z = 0$;

(ii) a dislocation $\dfrac{2\mu_1}{\mu_1 + \mu_2} b$ located at the moving singular point

$$z = \frac{z_0(R^2 - \rho\bar{\rho}\exp(\lambda t)) - \rho R^2(1 - \exp(\lambda t))}{(R^2 \exp(\lambda t) - \rho\bar{\rho}) - z_0\bar{\rho}(\exp(\lambda t) - 1)},$$

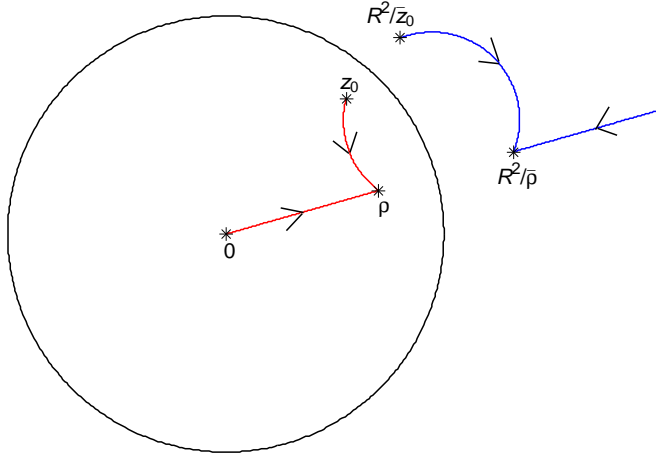which originates from $z = z_0$ and moves toward $z = \rho$;

Figure 5. Loci of the moving image dislocations when the original dislocation is located inside the inclusion. The image dislocations outside the circle $r = R$ are those for the inclusion; those within the circle $r = R$ are for the matrix.

(iii) a dislocation $-\dfrac{2\mu_1}{\mu_1 + \mu_2} b$ located at the moving singular point

$$z = \frac{\rho R^2 (\exp(\lambda t) - 1)}{R^2 \exp(\lambda t) - \rho \bar{\rho}},$$

which originates from $z = 0$ and moves toward $z = \rho$.

All four image dislocations are located within the inclusion. The two moving dislocations (or more precisely a moving dislocation dipole) will finally converge to the same point $z = \rho$, as also illustrated in Figure 5. The sum of these three dislocations is b.

5.2. *Uniform eigenstrains imposed on the inclusion.* When only uniform eigenstrains ε_{zx}^* and ε_{zy}^* are imposed on the circular inclusion, the two analytic functions can be finally derived as

$$f_1(z, t) = -\frac{2\mu_2(\varepsilon_{zy}^* + i\varepsilon_{zx}^*)}{\mu_1 + \mu_2} \frac{z(R^2 \exp(-\lambda t) - \rho \bar{\rho}) + \rho R^2(1 - \exp(-\lambda t))}{z\bar{\rho}(\exp(-\lambda t) - 1) + R^2 - \rho \bar{\rho} \exp(-\lambda t)} \qquad (|z| < R), \qquad (38)$$

$$f_2(z, t) = -\frac{2\mu_1(\varepsilon_{zy}^* - i\varepsilon_{zx}^*)}{\mu_1 + \mu_2} \frac{z\bar{\rho} R^2(1 - \exp(-\lambda t)) + R^2(R^2 \exp(-\lambda t) - \rho \bar{\rho})}{z(R^2 - \rho \bar{\rho} \exp(-\lambda t)) + R^2 \rho(\exp(-\lambda t) - 1)} \qquad (|z| > R). \qquad (39)$$

It is observed that the internal stress field is also nonuniform when uniform eigenstrains are imposed on the inclusion with a nonuniform viscous interface.

6. Conclusions

We obtained closed-form solutions in terms of elementary functions for a circular elastic inclusion bonded to an infinite elastic matrix through a circumferentially inhomogeneous viscous interface. Here the interface drag parameter takes the special form $1/\beta(\theta) = a_0 + a_1 e^{i\theta} + \bar{a}_1 e^{-i\theta}$, which can grasp the main feature of the nonuniformity of the interface.

We first obtained the general solutions for an arbitrary type singularity located in the matrix. Then the general solutions were applied to two specific loading cases: when the matrix is subjected to remote uniform shearing, and when a screw dislocation is located in the matrix. The effective shear modulus was obtained using the Mori–Tanaka method. We also interpreted the obtained dislocation solution in terms of image moving and static dislocations.

We then discussed other two loading conditions: a screw dislocation inside the inclusion, and uniform eigenstrains imposed on the inclusion.

The dislocation solutions obtained in this research can be easily applied to study a curved or a straight crack interacting with the inclusion [Cheeseman and Santare 2000; 2001].

Acknowledgement

References

[Cheeseman and Santare 2000] B. A. Cheeseman and M. H. Santare, "The interaction of a curved crack with a circular elastic inclusion", *Int. J. Fract.* **103**:3 (2000), 259–277.

[Cheeseman and Santare 2001] B. A. Cheeseman and M. H. Santare, "The effect of the interphase on crack-inclusion interactions", *Int. J. Fract.* **109**:3 (2001), 303–323.

[Dundurs 1967] J. Dundurs, "On the interaction of a screw dislocation with inhomogeneities", pp. 223–233 in *Recent advances in engineering science*, vol. 2, edited by A. C. Eringen, Gordon and Breach, 1967.

[Fan and Wang 2003] H. Fan and G. F. Wang, "Interaction between a screw dislocation and viscoelastic interfaces", *Int. J. Solids Struct.* **40**:4 (2003), 763–776.

[Frost and Ashby 1982] H. J. Frost and M. F. Ashby, *Deformation-mechanism maps*, Pergamon Press, Oxford, 1982.

[He and Lim 2001] L. H. He and C. W. Lim, "Time-dependent interfacial sliding in fiber composites under longitudinal shear", *Compos. Sci. Technol.* **61**:4 (2001), 579–584.

[Kim and McMeeking 1995] K. T. Kim and R. M. McMeeking, "Power law creep with interface slip and diffusion in a composite material", *Mech. Mater.* **20**:2 (1995), 153–164.

[Lazar 2007] M. Lazar, "On the screw dislocation in a functionally graded material", *Mech. Res. Commun.* **34**:3 (2007), 305–311.

[Mori and Tanaka 1973] T. Mori and K. Tanaka, "Average stress in matrix and average elastic energy of materials with misfitting inclusions", *Acta Metall.* **21**:5 (1973), 571–574.

[Ru 1999] C. Q. Ru, "Three-phase elliptical inclusions with internaluniform hydrostatic stresses", *J. Mech. Phys. Solids* **47**:2 (1999), 259–273.

[Ru and Schiavone 1997] C. Q. Ru and P. Schiavone, "A circular inclusion with circumferentially inhomogeneous interface in antiplane shear", *Proc. R. Soc. Lond. A* **453** (1997), 2551–2572.

[Wang et al. 2008] X. Wang, E. Pan, and A. K. Roy, "Interaction between a screw dislocation and a piezoelectric circular inclusion with viscous interface", *J. Mech. Mater. Struct.* **3**:4 (2008), 761–773.

XU WANG: xuwang@uakron.edu
University of Delaware, Center for Composite Materials, 202 Composites Manufacturing Science Laboratory, Newark, DE 19716, United States